Corrosion resistance and catalytic activity of nickel coatings electrodeposited from a chloride-glycinate electrolyte with the addition of thiourea

O.A. Kozaderov, L.V. Yudenkova and N.V. Sotskaya*

Voronezh State University, Universitetskaya pl. 1, 394018 Voronezh, Russian Federation
**E-mail: nvs@chem.vsu.ru*

Abstract

Electrolytic nickel deposition is one of the most widely used electroplating processes for obtaining functional Ni-coatings. Depending on the required properties, various surfactants are introduced into the deposition electrolytes, acting as brighteners, levellers, wetting agents (anti-pitting additives), as well as contributing to the chemical modification of the coating surface by introducing heteroatoms into their composition. Thiourea is characterized by a strong adsorption interaction with the nickel surface, which contributes to the inclusion of sulfur in the composition of coatings and variation of their properties. Nickel alloys containing sulfur are widely used in the electroplating industry and are also promising materials for the electrolytic production of hydrogen. However, the corrosion potential and passivation ability of nickel alloys containing sulfur are relatively low, that is why it is important to study their corrosion resistance in combination with other characteristics. In this paper, the effect of thiourea on the catalytic activity and corrosion properties of nickel coatings electrodeposited from a chloride-glycinate electrolyte is studied. It was found that coatings obtained in the presence of thiourea are characterized by the presence of cracks on the surface regardless of the concentration of the additive, an increase in which contributes to a decrease in the size of the crystallites. It is shown that with an increase in the content of thiourea in the glycinate electrolyte, the sulfur content in the coating increases, which becomes morphologically more developed, and due to the amorphization of the sulfur-containing deposit, more ductile. The rate of hydrogen evolution reaction in sulfuric acid solution increases with increasing coating thickness and with the inclusion of sulfur in its composition, which indicates the electrocatalytic properties of synthesized materials. However, the open-circuit potential of Ni-coatings with various thicknesses is about 0.2 V more negative than compact nickel, and the addition of thiourea further shifts its value to the more cathodic values. The introduction of sulfur into the nickel coating contributes to an increase in the rate of corrosion, while systems containing 9−11 wt.% S are optimal in terms of corrosion resistance in a sulfuric acid solution and high catalytic activity in the hydrogen evolution reaction.

Received: April 1, 2024. Published: May 31, 2024 doi: 10.17675/2305-6894-2024-13-2-21

Keywords: *electrochemical deposition, nickel, thiourea, corrosion.*

Introduction

Electrolytic nickel deposition is one of the most widely used processes in electroplating. Nickel is used to cover products made of steel and non-ferrous metals for corrosion protection and decorative surface finishing, and is also used as functional coatings, including in microelectronics. An electrochemical deposition of nickel coatings is a promising method for creation of microelectromechanical systems (MEMS) consisting of mechanical elements, sensors, actuators and microelectronic devices located on a common silicon substrate [1–4].

Depending on the required structural, mechanical and morphological properties of the galvanic Ni-coating, various additives to the base electrolytes of nickel plating are used. The most common are organic surfactants [5]. Adsorbed on the cathode surface, they are able to influence the formation and growth of a new phase of the deposit, inhibit the hydrogen evolution reaction, and reduce the mechanical stresses of the deposit. In addition, organic additives act as levelers, brighteners, wetting agents, which contributes to the production of coatings with the necessary morphology, structure and composition. Nickel plating electrolytes containing amino acids, for example, glycine [6], are non-toxic and contribute to the formation of stable complexes with nickel ions.

It was previously shown that thiourea $CS(NH_2)_2$ is a multifunctional organic additive in the electrodeposition of nickel from sulfate-chloride electrolytes, increasing cathodic polarization and reducing the differential capacitance of the double electric layer [7], acting as a brightener and leveler when varying the concentration and density of the deposition current [8–11], and when introduced into an ammonium electrolyte, it changes the grain size in such a way that it allows to obtain a homogeneous and fine-crystalline nickel deposit [12].

Under certain conditions, thiourea is used to produce electrode materials modified with sulfur, which is easily incorporated into nickel coatings due to the strong adsorption properties of $CS(NH_2)_2$ and its subsequent effect on the characteristics of the electrode/solution interface. Nickel alloys containing sulfur are widely used in the electroplating industry due to their relatively low dissolution potential and lack of passivation on the surface [13]. In addition, Ni-S alloys attract attention as a potential material for the creation of electrocatalysts for the hydrogen [14–18] or oxygen [19] evolution reaction, electrode materials for supercapacitors and batteries [20], solar panels [21]. This is due to an increase in the catalytic activity of the nickel coating when sulfur is introduced into its composition. However, the corrosion resistance of such S-containing coatings decreases [5], which requires solving a complex problem of determining the composition of the electrolyte to obtain Ni-coatings with an optimal ratio of corrosion and electrochemical characteristics.

The purpose of this work is to establish the role of thiourea in the formation of morphology, chemical composition, structure, mechanical properties, catalytic activity and corrosion resistance of nickel coatings electrodeposited from a chloride-glycinate electrolyte.

Experimental

Electrochemical deposition of nickel coatings of various thicknesses (1–5 microns) was carried out on a copper electrode in a standard three-electrode cell made of a chloride–glycinate electrolyte of the following composition: 0.08 M $NiCl_2 \cdot 6H_2O$ + 0.20 M HGly + *x* M $CS(NH_2)_2$ ($x = 0-10^{-2}$) at pH=5.5. The solutions were prepared on distilled water by sequential dissolution of nickel chloride, glycine and thiourea of reagent and analytical grade. The pH value was adjusted by adding a 10% NaOH solution and controlled potentiometrically using a glass electrode and a universal ionomer IPL-111. Before deposition, the copper electrode was grinded with sandpapers with decreasing grain size, then polished with soft suede and degreased with ethyl alcohol. After each operation, the electrode was thoroughly rinsed with distilled water and dried with filter paper. The reference electrode was a saturated silver chloride electrode, an auxiliary one was a platinum plate. Cathodic deposition was carried out at room temperature in a potentiostatic mode at $E = -1.00$ V using an IPC-Compact potentiostat. The potential chosen corresponds to the peak on the cathodic polarization curves in this electrolyte [6]. The potential values *E* are given in the paper on the scale of the standard hydrogen electrode.

The thickness of the coatings was calculated using the formula:

$$h = \frac{I \cdot M \cdot \tau}{z \cdot F \cdot S_{\text{geom}} \cdot \rho} \cdot 10^4, \quad (1)$$

where *I* – current (A); *M* – molar mass of nickel (59 g/mole); τ – deposition duration (s); *z* – number of electrons ($z = 2$); *F* – Faraday constant (96485 C/mole); S_{geom} – geometric area of the electrode (cm^2); ρ – nickel density (8.9 g/cm^3).

The current efficiency was calculated from gravimetric data using the formula:

$$CE = \frac{m_{\text{fact}}}{\left(IM\tau / zF\right)} \cdot 100\%, \quad (2)$$

where m_{fact} – mass of the cathodic deposit.

The surface morphology and composition of electrodeposited Ni-coatings were studied using scanning electron microscopy (SEM) on a JSM-6380LV device (JEOL Ltd.) equipped with an INCA Energy 250 X-Ray spectral microanalysis system (Oxford Instruments).

The phase composition of the coatings was determined by X-Ray diffraction analysis on an Empyrean B.V. (PANalytica) diffractometer (Cu K_α-radiation, 35 kV, 30 mA). To quantify the structure and crystallographic orientation of the *hkl*-faces of nickel crystallites, the relative texture coefficient RTC_{hkl} was calculated using the formula:

$$RTC_{hkl} = \frac{I^{hkl}}{\sum I^{hkl}} \times 100\%, \quad (3)$$

where I^{hkl} – the diffraction intensity of the crystallographic *hkl*-plane. The grain sizes of the crystallites were found by the Debye–Scherrer equation:

$$d = \frac{0.9\lambda}{b\cos\theta}, \tag{4}$$

where θ is the diffraction angle, λ is the wavelength of the X-Ray radiation, *b* is the width of the peak at half the height. The results of electron microscopic, X-Ray spectral and X-Ray diffraction studies were obtained on the equipment of the Voronezh State University Centre for the Collective Use of Scientific Equipment.

The study of the corrosion-electrochemical behavior of nickel coatings was carried out by a potentiodynamic method using a computerized potentiostat-galvanostat IPC-Compact in a standard three-electrode cell. A copper electrode with pre-deposited coatings of various thicknesses and with different sulfur content was used as a working electrode. The reference electrode was a saturated silver chloride electrode, an auxiliary one was a platinum plate. To determine the rate of hydrogen evolution reaction on synthesized Ni-coatings and to study their corrosive behavior, polarization curves were recorded at a potential scan rate of 10 mV/s in an argon-deaerated 0.05 M H_2SO_4 solution.

The current density was calculated for the geometric surface area of the electrode. To account for the surface development during electrodeposition, the values of the relative roughness factor f_r were used, which shows how many times the surface area of the coating differs from the surface area of a compact nickel electrode. The f_r value was found by the open-circuit chronopotentiometry as follows. At a given current density (–0.67 mA/cm^2), the pre-coated electrode was maintained for 400 s in a deaerated solution of 0.05 M H_2SO_4 until a constant overpotential ($\eta \approx \text{const}$) was established. Then, in an open-circuit state, an overpotential decay in time down to $\eta \approx 0$ was recorded. The corresponding curves $\eta - t$ were processed according to [22] to obtain the atomic hydrogen pseudo-adsorption capacity:

$$C_H\left[\eta(0)\right] = -\frac{i\left[\eta(0)\right]}{d\eta/dt\big|_{i_c;t\to 0}}, \tag{5}$$

according to the values of which the C_H,η-dependence was constructed and the charge of hydrogen adsorption Q_H was found on compact nickel and Ni-coatings. The roughness factor of the coatings in relation to a compact nickel electrode was estimated by the formula:

$$f_r = \frac{Q_H\left(\text{Ni}_{\text{coating}}\right)}{Q_H\left(\text{Ni}_{\text{compact}}\right)}. \tag{6}$$

The nanohardness of the obtained Ni-coatings was determined by the nanoindentation method on the NanoHardnessTester (CSM Instruments) device in the linear loading/unloading mode of the indenter. The loading rate was 9 mN/s, exposure time at maximum load was 1 s, and the unloading rate was 12 mN/s. The Meyer hardness (7) and Young's modulus (8) of the coatings were determined by the Oliver–Pharr method [23]:

$$\frac{P}{S^2} = \frac{\pi}{(2\beta)^2}\frac{H}{E_Y^2}, \quad (7)$$

$$E_Y = \frac{S\sqrt{\pi}}{2\beta\sqrt{A_c}}. \quad (8)$$

Here P is the load, S is the contact stiffness, β is the correction factor, H is the hardness, E_Y is the Young's modulus, A_c is the contact surface between the tip and the base.

Results and Discussion

General characteristics of coatings

SEM images of nickel coatings deposited from a chloride–glycinate electrolyte with different thiourea content are shown in Figure 1. It can be seen that all coatings are characterized by the presence of cracks, the number and severity of which increases with increasing concentration of $CS(NH_2)_2$. In this case, the coating obtained from a solution with a thiourea content of 1 mM is generally the smoothest. The scanning electron microscopy data are consistent with the results of determining the relative roughness factor (Table 1). Regardless of the coating thickness, the f_r parameter takes the value ~4–6 in the absence of thiourea in the electrolyte, while with the addition of 10^{-3} M $CS(NH_2)_2$ decreases to 1.5, and when thiourea is introduced into a solution at a concentration of $5\cdot10^{-3}$ M or more, it increases sharply to 9.

Table 1. Current efficiency (*CE*) and relative roughness factor (f_r) of Ni-coatings of different thickness (h), deposited from 0.08 M $NiCl_2\cdot6H_2O$ + 0.20 M HGly + x M $CS(NH_2)_2$.

x	h, μm	*CE*, %	f_r
0	1.06	66±3	4.48±0.13
0	2.08	65±2	4.24±0.08
0	3.06	75±4	4.54±0.18
0	3.98	73±3	5.92±0.18
0	5.04	65±4	5.22±0.21
10^{-3}	2.40	77±2	1.49±0.03
$5\cdot10^{-3}$	2.03	69±1	9.00±0.09
10^{-2}	2.20	76±3	8.70±0.26

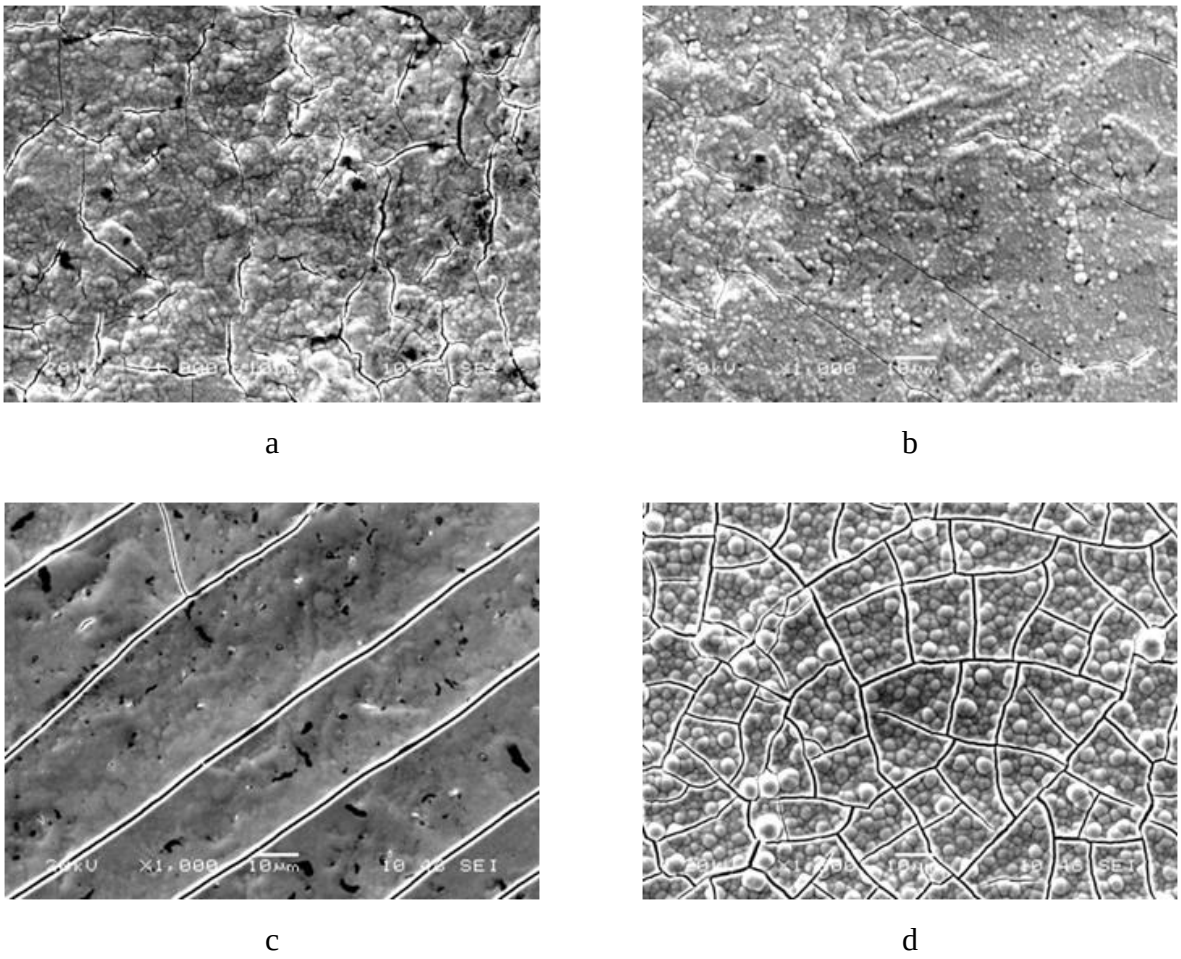

Figure 1. SEM micrographs (magnification ×1000) Ni-coatings deposited from 0.08 M $NiCl_2 \cdot 6H_2O$ + 0.20 M HGly + *x* M $CS(NH_2)_2$ with different concentration of thiourea *x* = 0 (a), $1 \cdot 10^{-5}$ (b), $1 \cdot 10^{-3}$ (c), $1 \cdot 10^{-2}$ (d).

Since the nickel electrodeposition proceeds in parallel with the hydrogen evolution reaction, the current efficiency takes a value from 65 to 77%, which varies slightly with variations in both the coating thickness and the thiourea content in the electrolyte.

Using energy-dispersive X-Ray spectroscopy, it was found that when thiourea is introduced into the nickel plating electrolyte, starting from a concentration of $1 \cdot 10^{-3}$ M, sulfur is incorporated into the coating (Table 2). Moreover, the higher the $CS(NH_2)_2$ content in the solution, the higher the S content in the coating. Comparison with data on roughness factors and SEM micrographs leads to the conclusion that the introduction of sulfur into the coating at a concentration of 1.73 wt.% smoothens the surface compared to a sulfur-free Ni-coating, while a further increase in the concentration of S leads to the development of the surface.

Table 2. Elemental composition (wt.%) of the coatings deposited from 0.08 M $NiCl_2 \cdot 6H_2O$ + 0.20 M HGly + *x* M $CS(NH_2)_2$.

x	Ni	S	O
0	96.04±0.20	–	3.96±0.20
$1 \cdot 10^{-5}$	95.85±0.19	–	4.15±0.19
$1 \cdot 10^{-3}$	96.53±0.18	1.73±0.09	1.75±0.16
$5 \cdot 10^{-3}$	88.46±0.23	9.49±0.14	2.04±0.19
$1 \cdot 10^{-2}$	87.65±0.22	10.64±0.15	1.71±0.19

Diffractograms of nickel coatings obtained in the absence of a thiourea additive, as well as with its minimal content, are characterized by diffraction peaks for planes 111, 200 and 220 (Figure 2). At the same time, for solutions with an organic additive, the intensity of all these peaks is reduced. With a higher content of thiourea, the diffraction peaks of the faces 200 and 220 are absent.

Based on the X-Ray diffraction data obtained, nickel grain sizes and relative texture coefficient were calculated (Table 3). It can be seen that with an increase in the concentration of the $CS(NH_2)_2$ additive, the grain size decreases, and for all the coatings obtained, the orientation of the faces 111 is mainly observed, which is consistent with the data [12, 24].

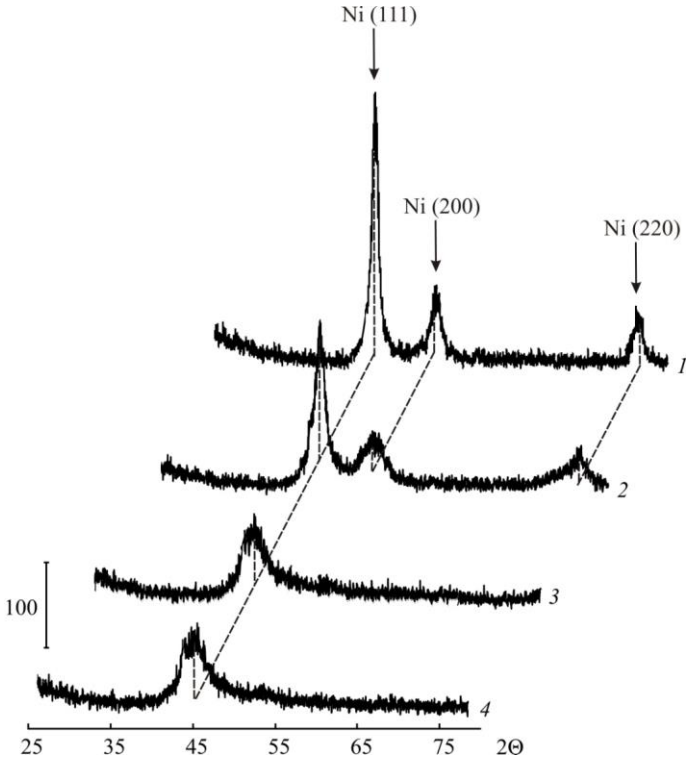

Figure 2. Diffractograms of Ni-coatings deposited from 0.08 M $NiCl_2 \cdot 6H_2O$ + 0.20 M HGly + *x* M $CS(NH_2)_2$ with the different concentration of thiourea $x = 0$ (1), $1 \cdot 10^{-5}$ (2), $1 \cdot 10^{-3}$ (3), $1 \cdot 10^{-2}$ (4).

Table 3. Crystallite size (d_{hkl}) and relative texture coefficient (RTC_{hkl}) for the coatings deposited from 0.08 M $NiCl_2 \cdot 6H_2O$ + 0.20 M HGly + *x* M $CS(NH_2)_2$.

x	d_{111}, nm	d_{200}, nm	d_{220}, nm	RTC_{111}, %	RTC_{200}, %
0	8.85	6.60	7.50	70.5	17.6
$1 \cdot 10^{-3}$	5.37	5.82	6.02	69.4	16.5
$5 \cdot 10^{-3}$	2.96	–	–	100	–
$1 \cdot 10^{-2}$	3.44	–	–	100	–

The data of X-Ray diffraction analysis correlate with the results of nanoindentation. Figure 3 shows diagrams of the load (*P*) – penetration depth (*h*) of the indenter. The results of the calculation of the main mechanical properties – hardness and modulus of elasticity – for the studied systems are presented in Table 4. It follows from these data that the deformation of the samples is elastoplastic. The changes in hardness and modulus of elasticity of the obtained coatings are non-monotonic. Relatively high values of *P* and E_Y indicate the crystallinity of coatings obtained from electrolytes without thiourea. On the contrary, for S-containing coatings, a sharp decrease in hardness is observed, which, with the broadening of diffraction peaks (Figure 2), indicates amorphization of the structure and suggests a relatively low corrosion resistance.

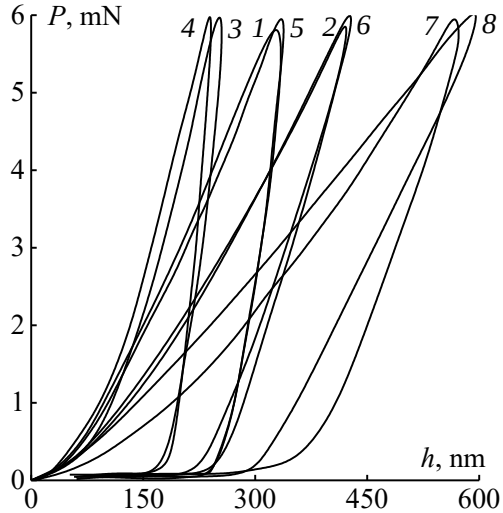

Figure 3. Load – indenter penetration depth diagrams for Ni-coatings of various thicknesses: 1 (2), 2 (3, 7, 8), 3 (4), 4 (5), 5 μm (6) and with different content of sulfur (wt.%): 0 (1–6), 1.7 (7), 9.5 (8).

Catalytic activity and corrosion resistance of coatings

To evaluate the catalytic effect in the hydrogen evolution reaction on Ni-coatings deposited from electrolytes with different thiourea contents, the cathodic branches of polarization curves obtained in 0.05 M H_2SO_4 were analyzed (Figure 4a). The current density at

E=−0.3 V (corresponding to the potential region common to all obtained curves) was taken as a measure of the hydrogen evolution reaction. It can be seen that all the obtained alloys have higher cathodic currents compared with compact nickel. At the same time, the greater the thickness of the coating, the effect is generally more pronounced. The inclusion of sulfur in the coating also contributes to an increase in the cathodic current density.

To correctly estimate the rate of hydrogen evolution reaction, the effect of coating surface development was taken into account, normalizing the found values of cathodic current density by the relative roughness factor of the coatings (Table 1). The analysis of the corrected values (Figure 4b) confirms an increase in catalytic activity only for sulfur-containing Ni-coatings, since despite the decrease in current density after normalization, it remains higher than on a compact nickel electrode. The coating with a sulfur content of 1.7 wt.% exhibits the highest catalytic activity. It can be explained by the smoothing of the surface compared to the nickel coating, as well as the lowest roughness factor among S-containing coatings (Table 1). In addition, it is the coating with a minimum sulfur content that, according to diffractometric data, is polycrystalline (Table 3), which probably also contributes to an increase in catalytic activity.

The corrosion resistance of the synthesized catalytically active Ni-coatings in 0.05 M H_2SO_4 was evaluated using full polarization curves (Figure 4a), determining the corrosion potential of the E_{corr}, Tafel slopes b_a and b_c, (Table 5), as well as the corrosion current density i_{corr} (Figure 4c).

Table 5. Corrosion potential (E_{corr}) and Tafel slopes of cathodic (b_c) and anodic (b_a) linear branches of the polarization curves in 0.05 M H_2SO_4 on Ni-coatings deposited from 0.08 M $NiCl_2 \cdot 6H_2O$ + 0.20 M HGly + x M $CS(NH_2)_2$ in dependence on the thickness (h) and sulfur content (ω_S)

Electrode	x	h, μm	ω_S, wt.%	b_c, V	b_a, V	E_{corr}, V
Ni compact	–	–	–	–0.045	0.044	0.071
Ni-coating	0	1.06	0	–0.038	0.039	–0.103
	0	2.08	0	–0.048	0.042	–0.102
	0	3.06	0	–0.052	0.041	–0.095
	0	3.98	0	–0.043	0.041	–0.109
	0	5.04	0	–0.046	0.038	–0.104
	10^{-3}	2.40	1.7	–0.047	0.040	–0.167
	$5 \cdot 10^{-3}$	2.03	9.5	–0.045	0.046	–0.200
	10^{-2}	2.20	10.6	–0.043	0.048	–0.197

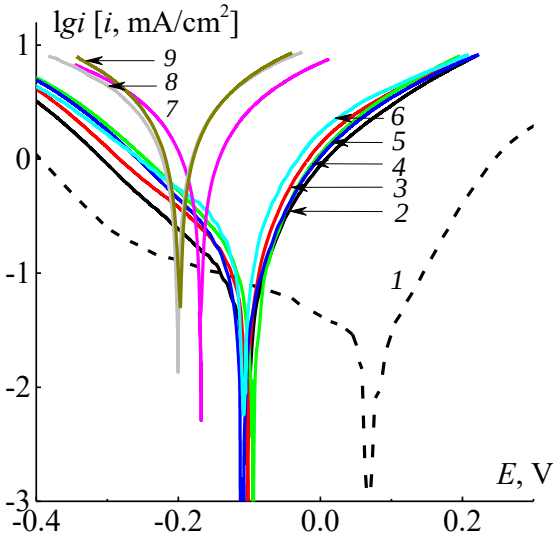

a

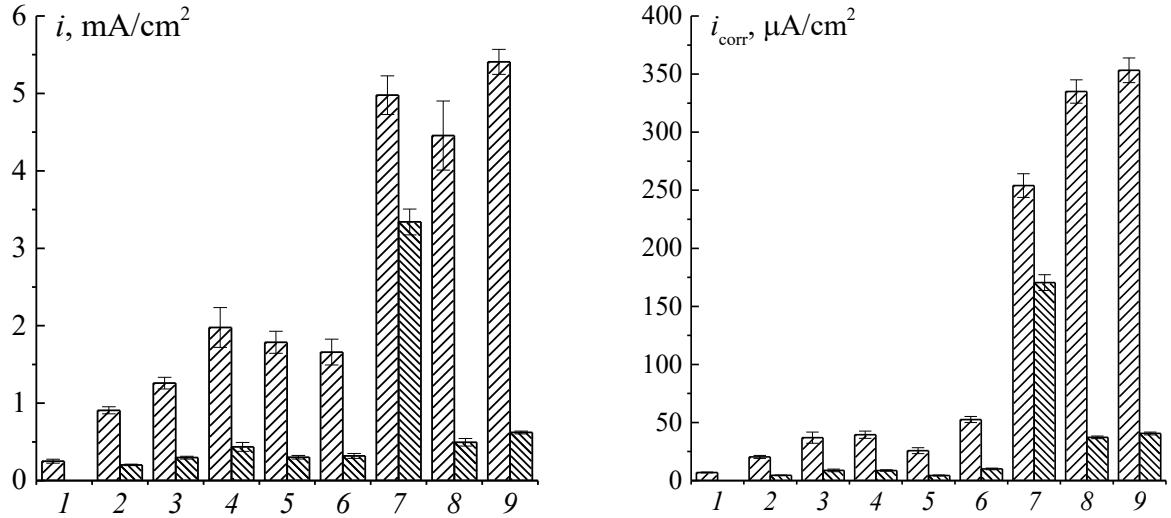

b c

Figure 4. Polarization curves (*a*), hydrogen evolution reaction rate at –0.3 V (*b*) and corrosion current density (c) in 0.05 M H_2SO_4 on compact nickel (1) and electrodeposited Ni-coatings with different thickness (μm): 1 (2), 2 (3, 7–9), 3 (4), 4 (5), 5 (6), and different sulfur content (wt.%): 0 (1–6), 1.7 (7), 9.5 (8), 10.6 (9), calculated without (▨) and with (▩) taking into account of the relative roughness factor.

The corrosion potential E_{corr} of nickel coatings of various thicknesses turned out to be approximately 0.2 V negative compared to compact nickel. When thiourea is added to the electrolyte solution and sulfur is introduced into the coating composition, the E_{corr} is even more strongly shifted to the cathodic region.

Comparing the values of the Tafel slopes (Table 5) with the literature data, it can be assumed that the limiting stage of the cathodic process is the electrochemical desorption.

Indeed, if the formation of molecular hydrogen proceeds by the mechanism of "electrochemical" recombination of discharged hydrogen ions with atomic hydrogen presented on the surface:

$$H_{ads} + H_3O^+_{ads} + e \rightarrow H_2 + H_2O, \quad (9)$$

then the Tafel slope takes the value $b_c \approx -0.040$ V, with which the data obtained in our work are consistent (Table 5). For the anodic process near the corrosion potential, taking into account the values of $b_a \approx 0.040$ V, the stage of cleavage of the second electron can be stated as limiting step. The nature of the limiting stage of cathodic and anodic reactions does not change during the transition from compact nickel to electroplated coatings and after inclusion of sulfur in their composition. However, the polarization curves shift towards higher currents, which indicates an acceleration of both the cathodic and anodic processes on synthesized coatings. As a result, the transition from compact nickel to Ni-coatings, as well as an increase in its sulfur content, leads to an increase in the corrosion current density. Such effects can be caused both by a change in the electronic structure of nickel during alloying with a non-metal, and by the observed change in the surface area of the coating compared with compact nickel (Figure 1, Table 1). However, if, after correction on the relative roughness factor, the values of i_{corr} for compact nickel and coatings are practically the same, then the corrosion rate of sulfur-containing Ni-coatings remains relatively high compared to compact nickel even after taking into account surface development (Figure 4c). In addition, the i_{corr} value is higher for the lower sulfur content in the coating. Indeed, the corrosion rate is maximum for an alloy with a sulfur content of 1.7 wt.%, characterized by the smoothest surface, which is consistent with its highest catalytic activity with respect to cathodic reduction of hydrogen. In turn, on alloys with the non-metal content of 9.5 and 10.7 wt.% the main contribution to the observed increase in corrosion current is mainly due to surface development. Thus, nickel coatings with a sulfur content of 9–11 wt.% are optimal in composition in terms of corrosion resistance in a sulfuric acid solution and high catalytic activity in relation to the hydrogen evolution reaction.

Conclusion

Nickel coatings electrochemically deposited from a chloride-glycinate electrolyte with a different content of thiourea are rough. The degree of morphological development of the coating surface slightly depends on their thickness, decreases markedly with the addition of 1 mM $CS(NH_2)_2$ and increases sharply with a further increase in the concentration of the organic additive to 10 mM. The current efficiency varies slightly with changes in the thickness of the coating and the content of thiourea in the electrolyte, and it is less than 80%, which can be explained by the side process of hydrogen evolution.

When thiourea is introduced into the nickel deposition electrolyte, starting from a concentration of 1 mM, sulfur is incorporated into the coating, the content of which increases with an increase in the concentration of $CS(NH_2)_2$ in the electrolyte. The introduction of sulfur into the coating at a concentration of 1.73 wt.% leads to a smoothing of the surface; a

further increase in the concentration of S contributes to its morphological development. With an increase in the concentration of the additive, the size of the crystallites decreases, and for all the obtained coatings, the (111) orientation of the faces is mainly observed.

Relatively high values of hardness and modulus of elasticity indicate the crystallinity of coatings obtained from electrolytes without thiourea, while sulfur-containing systems are characterized by amorphization of their structure.

An analysis of the cathodic process rate in a sulfuric acid solution, normalized by the degree of surface development, confirms an increase in the catalytic activity of sulfur-containing Ni-coatings in the hydrogen evolution reaction compared with compact nickel. The coating with a sulfur content of 1.7 wt.% exhibits the greatest catalytic activity. The limiting stage of the cathodic process is electrochemical desorption of hydrogen.

The corrosion potential of the obtained nickel coatings of various thicknesses is noticeably shifted in the negative direction compared with compact nickel. The shift is manifested to a greater extent when thiourea is added to the electrolyte solution and sulfur is introduced into the coating composition. The anodic oxidation of nickel during corrosion of the coating in a sulfuric acid solution is controlled by the cleavage of the second electron.

Corrosion of compact nickel and synthesized Ni-coatings in a sulfuric acid solution proceeds at approximately the same rate. For sulfur-containing Ni-coatings, the corrosion rate is relatively high even after taking into account surface development and takes the lowest value for alloys with a non-metal content of 9.5 and 10.7 wt.%. These results can be used in electrolytic nickel plating to obtain functional Ni-coatings with an optimal ratio of catalytic activity and corrosion resistance.

Acknowledgements

The study received financial support from the Ministry of Science and Higher Education of the Russian Federation within the framework of the State Contract with the universities regarding scientific research in 2022–2024, project No. FZGU-2022-0003.

References

1. T. Xin and P.K. Ajmera, Nickel electrodeposition studies for high-aspect-ratio microstructure fabrication for MEMS, *Proc. SPIE*, 2006, **6172**, 104–113. doi: 10.1117/12.659104
2. G. Ding, Y. Zhang, J. Liu, X. Zhao, B. Cai and T. Shen, Electrochemical studies of electrodeposition of nickel for LIGA microstructures, *Proc SPIE*, 2001, **4601**, 306–311. doi: 10.1117/12.444706
3. P. Prioteasa, A. Petica, M. Popa, C.I. Ilie and T. Visan, Electrochemical deposition of nickel for micro-mechanical systems, *Revista de Chimie*, 2011, **62**, no. 5, 543–548.
4. T.E. Buchheit, J.R. Michael, T.R. Christenson, D.A. LaVan and S.D. Leith, Microstructural and mechanical properties investigation of electrodeposited and annealed LIGA nickel structures, *Metall Mater. Trans. A*, 2002, **33**, 539–554. doi: 10.1007/s11661-002-0116-3

5. U.S. Mohanty, B.C. Tripathy, P. Singh, A. Keshavarz and S. Iglauer, Roles of organic and inorganic additives on the surface quality, morphology, and polarization behavior during nickel electrodeposition from various baths: a review, *J. Appl. Electrochem.*, 2019, **49**, 847–870. doi: 10.1007/s10800-019-01335-w
6. N.V. Sotskaya and O.V. Dolgikh, Nickel electroplating from glycine containing baths with different pH, *Prot. Met.*, 2008, **44**, 479–486. doi: 10.1134/S0033173208050123
7. S.S. Kruglikov, N.T. Kudryavtsev and R.P. Sobolev, The effect of some primary and secondary brighteners on the double layer capacitance in nickel electrodeposition, *Electrochim. Acta*, 1967, **12**, no. 9, 1263–1271. doi: 10.1016/0013-4686(67)80043-4
8. G.T. Rogers, M.J. Ware and R.V. Fellows, The incorporation of sulfur in electrodeposited nickel, using thiourea as a brightener and leveler, *J. Electrochem. Soc.*, 1960, **107**, 677–682. doi: 10.1149/1.2427807
9. J.J. Hoekstra and D. Trivich, The uptake of sulfur from plating brighteners by copper and nickel, *J. Electrochem. Soc.*, 1964, **111**, 162–168. doi: 10.1149/1.2426076
10. B.N. Popov, Contribution to the knowledge of the electrodeposition of nickel in the presence of organic compounds, *Kem. Ind.*, 1982, **31**, 455–461.
11. U.S. Mohanty, B.C. Tripathy, S.C. Das and V.N. Misra, Effect of thiourea during nickel electrodeposition from acidic sulfate solutions, *Metall. Mater. Trans. B*, 2005, **36**, 737–741. doi: 10.1007/s11663-005-0077-1
12. L. Yuan, J. Hu, Z. Ding and S. Liu, Electrochemical deposition of bright nickel on titanium matrix from ammoniacal solution in the presence of thiourea, *Int. J. Electrochem. Sci.*, 2017, **12**, no. 8, 7312–7325. doi: 10.20964/2017.08.56.
13. H. Cao, D. Yang, Sh. Zhu, L. Dong and G. Zheng, Preparation, characterization, and electrochemical studies of sulfur-bearing nickel in an ammoniacal electrolyte: the influence of thiourea, *J. Solid State Electrochem.*, 2012, **16**, 3115–3122. doi: 10.1007/s10008-012-1753-0
14. M. Prigent, L.J. Mas and F.C. Verillon, *Proceedings, Symposium on Industrial Water Electrolysis*, Vol. 78−4, Edited by S. Srinivasan, The Electrochemical Society, Princeton, New Jersey, 1978, p. 234.
15. R. Sabela and I. Paseka, Properties of Ni-Sx electrodes for hydrogen evolution from alkaline medium, *J. Appl. Electrochem.*, 1990, **20**, 500–505. doi: 10.1007/BF01076063
16. L. Guo, Zh. Yuan, K. Jiao and X. Yu, Self-supporting porous Ni-S electrocatalyst with carbon doping for hydrogen evolution reaction, *Mater. Lett.*, 2021, **282**, 128651. doi: 10.1016/j.matlet.2020.128651
17. X. Li, Q. Li, W. Yan, B. Fan and Zh. Wang, In-situ controllable electrodeposition of NiS nanostructures coupled with polypyrrole for enhanced hydrogen evolution reaction, *Int. J. Hydrogen Energy*, 2024, **51**, 443–451. doi: 10.1016/j.ijhydene.2023.10.076
18. I.A. Poimenidis, M. Lykaki, N. Papakosta, P.A. Loukakos, N.K. Kontos and M. Konsolakis, One-step electrodeposition of NiS heterostructures on nickel foam electrodes for hydrogen evolution reaction: on the impact of thiourea content, *Results Chem.*, 2023, **6**, 101216. doi: 10.1016/j.rechem.2023.101216

19. H. Fan, Y. Ma, W. Chen, Y. Tang, L. Li and J. Wang, Facile one-step electrodeposition of two-dimensional nickel-iron bimetallic sulfides for efficient electrocatalytic oxygen evolution, *J. Alloys Compd*., 2021, **894**, 162533. doi: 10.1016/j.jallcom.2021.162533
20. T.N.J. Immanuel Edison, R. Atchudan, N. Karthik, K. Ganesh, D. Xiong and Y.R. Lee, A novel binder-free electro-synthesis of hierarchical nickel sulfide nanostructures on nickel foam as a battery-type electrode for hybrid-capacitors, *Fuel*, 2020, **276**, 118077. doi: 10.1016/j.fuel.2020.118077
21. Y. Xiao, Ch. Wang and G. Han, Effects of thiourea concentration on electrocatalytic performances of nickel sulfide counter electrodes for use in dye-sensitized solar cells, *Mater. Res. Bull*., 2015, **61**, 326–332. doi: 10.1016/j.materresbull.2014.10.052
22. B.E. Conway and L. Bai, Determination of the adsorption behaviour of 'overpotential-deposited' hydrogen-atom species in the cathodic hydrogen-evolution reaction by analysis of potential-relaxation transients, *J. Chem. Soc., Faraday Trans. 1*, 1985, **81**, 1841–1862. doi: 10.1039/F19858101841
23. W.C. Oliver and G.M. Pharr, An improved technique for determining hardness and elastic modulus using load and displacement sensing indentation experiments, *J. Mater. Res*., 1992, **7**, 1564–1583. doi: 10.1557/JMR.1992.1564
24. M.Y. Jung, Ch.S. Nam, B.-S. Lee and Y. Choi, Study on the effect of the thiourea on nano-mechanical properties and microstructures of the electroformed thin Ni-P foil, *Korean Journal of Metals and Materials*, 2020, **58**, no. 1, 1–6. doi: 10.3365/KJMM.2020.58.1.1

♦ ♦ ♦